RASĀYAN *J. Chem.*
Vol. 19 | No. 2 | 1017-1028| April-June | 2026
ISSN: 0974-1496 | e-ISSN: 0976-0083 | CODEN: RJCABP
http://www.rasayanjournal.com
http://www.rasayanjournal.co.in

PYTHON-BASED COMPUTATIONAL ANALYSIS AND VISUALIZATION OF VIBRATIONAL–ROTATIONAL BEHAVIOR IN SELECTED DIATOMIC MOLECULES

J. Singh[1], V. Wadhwa[2], and S. Bhattacharyya[1,✉]
[1]Department of Chemistry, Hansraj College, University of Delhi, Delhi-110007, (Delhi) India
[2]Department of Computer Science, Hansraj College, University of Delhi,
Delhi-110007, (Delhi) India
✉Corresponding author: shampa4@gmail.com

ABSTRACT
The vibrational and rotational motions of diatomic molecules play a crucial role in understanding their structural and spectroscopic properties. In the present study, a computational approach using Python has been developed to analyse various aspects of molecular vibrations within the harmonic and anharmonic oscillator frameworks. The potential energy variation with force constant was examined, and vibrational energies for several diatomic molecules (F–F, H–H, N–N, H–F, N–O, and C–O) were computed for different vibrational levels. The results show that the energy levels of the anharmonic oscillator are consistently lower than those of the harmonic oscillator and that the energy gap between successive levels decreases with increasing vibrational quantum number. The maximum vibrational quantum level, anharmonicity constant, and dissociation energy were also determined computationally. Furthermore, Boltzmann statistics were employed to evaluate the population distribution among vibrational and rotational energy levels at room temperature, revealing that the majority of molecules occupy the ground vibrational state. A novel computational visualization method has been proposed to represent energy levels, wave functions, and probability densities simultaneously on a single graphical scale. This integrated representation enhances the interpretation of quantum mechanical behaviour and provides an effective pedagogical tool for teaching molecular quantum mechanics using modern computational techniques.
Keywords: Python Programming, Quantum Mechanics, Vibrational Spectroscopy, Harmonic Oscillator, Anharmonic Oscillator, Diatomic Molecules, Computational Chemistry, Wave Function, Probability Density Visualization

RASĀYAN *J. Chem.*, Vol. 19, No.2, 2026

INTRODUCTION

Quantum mechanics provides the theoretical foundation for understanding the behavior of atoms and molecules at the microscopic scale. In molecular systems, vibrational and rotational motions play a significant role in determining spectroscopic properties, chemical bonding, and molecular stability. These motions are commonly described using the harmonic oscillator model, which provides a simplified but useful approximation for molecular vibrations. However, real molecular systems exhibit deviations from ideal harmonic behavior, and therefore, the anharmonic oscillator model is often required to provide a more accurate description of vibrational energy levels and molecular dissociation.[1-3] The mathematical treatment of such quantum mechanical systems often involves complex calculations that can be difficult to perform manually. With the rapid advancement of computational tools, programming languages such as Python have become powerful platforms for scientific computation and visualization. Python provides extensive libraries, such as NumPy, SciPy, Pandas, and Matplotlib, that enable efficient numerical calculations and graphical representation of scientific data.[4-5] Consequently, computational approaches have become increasingly important in chemical education and research, allowing students and researchers to better visualize abstract quantum mechanical concepts.[6-7] Several studies have applied computational methods to analyse vibrational and rotational energy levels of diatomic molecules. However, many existing studies primarily focus on numerical calculations without providing integrated graphical representations that combine energy levels, wave functions, and probability densities in a single coherent framework. This limitation makes it difficult for students and researchers to develop an intuitive

http://doi.org/10.31788/RJC.2026.1929626

understanding of the relationship between these quantum mechanical quantities. The present work aims to address this gap by developing a Python-based computational approach to analyse vibrational and rotational properties[8-9] of selected diatomic molecules, including F–F, H–H, N–N, H–F, N–O, and C–O. The study includes the computation of potential energy variations, vibrational energy levels for both harmonic and anharmonic oscillators, maximum vibrational quantum numbers, and Boltzmann population distributions. In addition, rotational population distributions in the ground vibrational state are evaluated. A novel visualization method is proposed that enables simultaneous representation of energy levels, wave functions, and probability densities on a single graphical scale, providing a clearer interpretation of molecular vibrational behaviour. This work also contributes to Sustainable Development Goal 4 (SDG-4: Quality Education) by integrating computational tools with fundamental concepts of quantum chemistry. The approach presented here supports modern teaching methodologies by enhancing students' analytical and computational skills while improving their conceptual understanding of molecular quantum mechanics.

Computational Details

The computational analysis has been performed on homonuclear (H-H, F-F, N-N) and heteronuclear (H-F, N-O, C-O) diatomic molecules. The paper links quantum mechanics and computational tools. In doing so, Python has been deployed to simulate and show the behavior of the Harmonic oscillator. NumPy, a powerful library for numerical computations, has been used to enable efficient handling of large arrays and mathematical operations. Pandas used in this paper provides flexible data structures like DataFrames for easy data cleaning, manipulation, and analysis. Matplotlib is used to create a wide range of interactive data visualizations to interpret results effectively.

RESULTS AND DISCUSSION

Effect of Force Constant on Potential Energy

The potential energy (V) of a diatomic molecule within the harmonic Oscillator approximation is given as:

$$V = \frac{1}{2} k x^2 \qquad (1)$$

where k represents force constant ($N m^{-1}$) and x represents the displacement from the equilibrium bond length. The potential energy curve obtained from this relation is parabolic, representing the restoring force acting on the vibrating atom. The computational results show that the shape of the potential energy curve strongly depends on the magnitude of the force constant. Molecules with large force constants exhibit deeper and narrower potential wells, indicating stronger bonding and higher vibrational frequencies. For example, the N–N molecule has a relatively large force constant, resulting in a steep and narrow potential well. In contrast, F–F has a smaller force constant and therefore has a wider and shallower potential energy curve (Table-1). Consequently, the potential energy curve of N-N is deep and narrow, whereas that of F-F is shallow and wide. A Python code (SI-Programme 1) is written to calculate the potential energy of the molecules. The result obtained is given in Table-2, and represented graphically in Fig.-1.

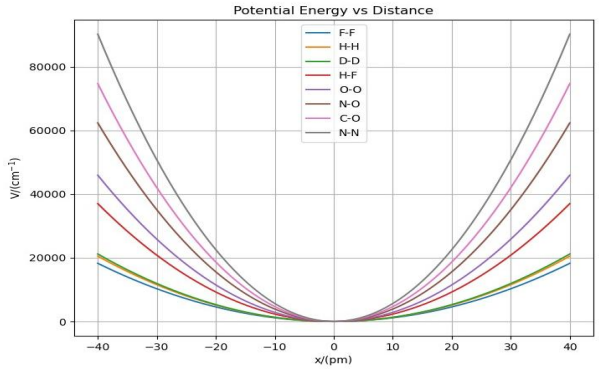

Fig.-1: Potential Energy (V) vs Internuclear Distance (x) with a different Force Constant (k).

Table-1: Spectroscopic Constants of a Diatomic Molecule [2]

Molecule	k/Nm^{-1}	$\tilde{\omega}_e/cm^{-1}$	$\tilde{x}_e\tilde{\omega}_e/cm^{-1}$
$F^{19}-F^{19}$	454	916.4	11.236
$H^{1}-H^{1}$	510	4403.56	123.86
$D^{2}-D^{2}$	527	3116.33	62.51
$O^{16}-O^{16}$	1142	1580.19	11.98
$N^{14}-N^{14}$	2243	2358.57	14.324
$H^{1}-F^{19}$	920	4138.32	89.88
$N^{14}-O^{16}$	1550	1904.2	14.075
$C^{12}-O^{16}$	1857	2169.81	13.288

Table-2: Variation of Potential Energy (V) with Force Constant (k)

x/pm	$v/cm^{-1} = 0.5kx^2$							
	F-F	H-H	D-D	H-F	O-O	N-O	C-O	N-N
-40	18268.7	20522.11	21206.18	37020.27	45953.42	62371.11	74724.61	90257.02
-30	10276.14	11543.60	11928.47	20823.9	25848.8	35083.75	42032.59	50769.57
-20	4567.174	5130.526	5301.544	9255.067	11488.36	15592.78	18681.15	22564.26
-10	1141.794	1282.632	1325.386	2313.767	2872.089	3898.194	4670.288	5641.064
0	0	0	0	0	0	0	0	0
10	1141.794	1282.632	1325.386	2313.767	2872.089	3898.194	4670.288	5641.064
20	4567.174	5130.526	5301.544	9255.067	11488.36	15592.78	18681.15	22564.26
30	10276.14	11543.60	11928.47	20823.9	25848.8	35083.75	42032.59	50769.57
40	18268.7	20522.11	21206.18	37020.27	45953.42	62371.11	74724.61	90257.02

Vibrational Energy at Different Vibrational Levels in Harmonic and Anharmonic Oscillators

The vibrational energies of the selected diatomic molecules were computed for several vibrational quantum numbers using both harmonic (HO) and anharmonic oscillator (AHO) models (equations 2 - 5).

$$E_{v_{HO}} = (v + 0.5)\tilde{\omega}_e \quad (2)$$

$$E_{v_{AO}} = (v + 0.5)\tilde{\omega}_e - \tilde{x}_e\tilde{\omega}_e(v + 0.5)^2 \quad (3)$$

$$\Delta E_{H0} = \tilde{\omega}_e \quad (4)$$

$$\Delta E_{AO} = \tilde{\omega}_e\left[1 - 2\tilde{x}_e(v + 1)\right] \quad (5)$$

where, v is a vibrational quantum number, $\tilde{\omega}_e$ is the wave number and $\tilde{x}_e$ is anharmonicity constant. The $\tilde{\omega}_e$ Some selected diatomic molecules are mentioned in Table-1.

Table-3: Computed Vibrational Energies (E_v/cm^{-1}) of Harmonic and Anharmonic Oscillator from v = 0 to 6

v	E_v/cm^{-1}					
	F-F		H-H		N-N	
	HO	AHO	HO	AHO	HO	AHO
0	458.2	455.39	2201.78	2170.82	1179.135	1175.554
1	1374.6	1349.32	6605.34	6326.65	3537.405	3505.176
2	2291.0	2220.78	11008.90	10234.78	5895.675	5806.15
3	3207.4	3069.76	15412.46	13895.18	8253.945	8078.476
4	4123.8	3896.27	19816.02	17307.85	10612.21	10322.15
5	5040.2	4700.31	24219.58	20472.82	12970.49	12537.18
6	5956.6	5481.88	28623.14	23390.06	15328.75	14723.57
v	E_v/cm^{-1}					
	H-F		N-O		C-O	

	HO	AHO	HO	AHO	HO	AHO
0	2069.16	2046.69	952.1	948.58	1084.905	1081.58
1	6207.48	6005.25	2856.3	2824.63	3254.715	3224.82
2	10345.80	9784.05	4760.5	4672.53	5424.525	5341.47
3	14484.12	13383.09	6664.7	6492.28	7594.335	7431.56
4	18622.44	16802.37	8568.9	8283.88	9764.145	9495.06
5	22760.76	20041.89	10473.1	10047.33	11933.96	11531.99
6	26899.08	23101.65	12377.3	11782.63	14103.77	13542.35

Table-4: Computed ΔE_{υ} of Harmonic and Anharmonic Oscillators

υ	ΔE_{υ}/cm^{-1}					
	F-F		H-H		N-N	
	HO	AHO	HO	AHO	HO	AHO
0-1	916.4	893.93	4403.56	4155.84	2358.27	2329.622
1-2	916.4	871.46	4403.56	3908.13	2358.27	2300.974
2-3	916.4	848.98	4403.56	3660.40	2358.27	2272.326
3-4	916.4	826.51	4403.56	3412.67	2358.27	2243.674
4-5	916.4	804.04	4403.56	3164.97	2358.27	2215.03
5-6	916.4	781.57	4403.56	2917.24	2358.27	2186.39
υ	ΔE_{υ}/cm^{-1}					
	H-F		N-O		C-O	
	HO	AHO	HO	AHO	HO	AHO
0-1	4138.32	3958.56	1904.2	1876.06	2169.81	2143.24
1-2	4138.32	3778.8	1904.2	1847.9	2169.81	2116.65
2-3	4138.32	3599.04	1904.2	1819.75	2169.81	2090.09
3-4	4138.32	3419.28	1904.2	1791.6	2169.81	2063.50
4-5	4138.32	3239.52	1904.2	1763.45	2169.81	2036.93
5-6	4138.32	3059.76	1904.2	1735.3	2169.81	2010.36

In the harmonic approximation, the energy levels increase linearly with the vibrational quantum number, and the spacing between adjacent levels remains constant. However, real molecular vibrations deviate from this ideal behavior. The anharmonic oscillator model provides a more realistic description of molecular vibrations. In this case, the energy of each vibrational level is slightly lower than that predicted by the harmonic oscillator model, and the spacing between successive vibrational levels gradually decreases as the quantum number increases. This trend reflects the weakening of the restoring force at larger internuclear separations, which ultimately leads to molecular dissociation. A Python code (SI-Programme 2) is written to calculate energy for six vibrational levels (υ = 0 to 6) for each of the diatomic molecules (F-F, H-H, N-N, H-F, N-O, and C-O). The results obtained are tabulated in Tables-3 and 4.

Determination of the Maximum Vibrational Level (υ_{max}) and the Anharmonicity Constant ($\breve{x}_e$) of the Molecule using the Anharmonic Oscillator Approach

The harmonic oscillator approximation is good only where the potential energy is a minimum. Its potential energy becomes infinite as x becomes very large. The idea of the dissociation of molecules is missing in this framework. Therefore, the maximum vibrational level (υ_{max}) is determined in the framework of anharmonic oscillator approximation. It is calculated under the condition that the energy gap (ΔE_{AO}) between two successive vibrational levels of anharmonic oscillator becomes zero, i.e.,

$$\Delta E_{AO} = E_{(\upsilon+1)_{AO}} - E_{\upsilon_{AO}} = 0.$$

Hence υ_{max} is determined from equation-5 and given in equation-6.

$$\upsilon_{max} = \frac{1}{2\tilde{x}_e} - 1 \qquad (6)$$

$$\tilde{x}_e = \frac{\tilde{\omega}_e \tilde{x}_e}{\tilde{\omega}_e} \qquad (7)$$

$$D_e = \frac{\tilde{\omega}_e}{4\tilde{x}_e} \qquad (8)$$

Python code (SI-Programme 3) is written to compute υ_{max}, $\tilde{x}_e$ and the dissociation energy (De). The results are given in Table-5.

Table-5: Computed Results of υ_{max}, $\tilde{x}_e$ and D_e

Molecule	υ_{max}		$\tilde{x}_e$		De kJ/mol
	Computed	Rounded off to an integer	Computed		Computed
$F^{19} - F^{19}$	39.779	40	1.2261E-02	-	223.7059
$H^{1} - H^{1}$	16.776	17	2.8127E-02	-	468.593
$D^{2} - D^{2}$	23.926	24	2.0059E-02	-	465.0037
$H^{1} - F^{19}$	22.02	22	2.1719E-02	(0.0218)[10]	570.3009
$O^{16} - O^{16}$	64.95	65	7.5814E-03	-	623.8509
$N^{14} - O^{16}$	66.64	67	7.3916E-03	(0.0073)[10]	771.0734
$C^{12} - O^{16}$	80.64	81	6.1240E-03	(0.0061)[10]	1060.481
$N^{14} - N^{14}$	81.32	81	6.0737E-03	-	1162.095

Population Distribution Among Various Vibrational Levels

The distribution of molecules among various energy levels follows the Boltzmann Distribution law. The total vibrational population (N_{Tot}) is calculated theoretically from $\upsilon = 0$ to υ_{max} for each molecule using both approaches so that the sum of the fractional populations approaches 1. The energy expression (E_υ) for Harmonic and Anharmonic oscillator, given in equations 6 and 7 respectively, have been used in equation-9 to calculate N_{Tot}. The N_{Tot} is expressed as:

$$N_{Tot} = \sum_{\upsilon=0}^{\upsilon_{max}} e^{\frac{-E_\upsilon}{kT}} g_\upsilon \qquad (9)$$

$$N_{Tot}^{HO} = \sum_{\upsilon=0}^{\upsilon_{max}} e^{\frac{-(\upsilon+0.5)\tilde{\omega}_e hc}{kT}} g_\upsilon \qquad (10)$$

$$N_{Tot}^{AO} = \sum_{\upsilon=0}^{\upsilon_{max}} e^{\frac{-((\upsilon+0.5)\tilde{\omega}_e - \tilde{x}_e\tilde{\omega}_e(\upsilon+0.5)^2)hc}{kT}} g_\upsilon \qquad (11)$$

Where, g_υ is the degeneracy of the vibrational level which is 1.

$$Normalised\ population, (P_\upsilon) = \frac{g_\upsilon exp^{-\frac{E_\upsilon hc}{kT}}}{N_{Tot}} \qquad (12)$$

A Python code (SI-Programme 4) is written to compute the fractional population in each vibrational level using equation 12. We calculated the normalized population from $\boldsymbol{\upsilon}$ = 0 to $\boldsymbol{\upsilon}$ = 6 instead of υ = 0 to

υ_{max} because the sum of these fractional populations is reaching 1. Hence, we avoided computing the same beyond $\boldsymbol{\upsilon}$ = 6. The result obtained is tabulated in Table-6 and represented graphically in Fig.-2. The vibrational population distribution graph remains the same with both approximations.

Table-6: Computed Normalized Population Distribution in Vibrational Levels, $\boldsymbol{\upsilon}$ = 0 to $\boldsymbol{\upsilon}$ = 6.

$\boldsymbol{\upsilon}$	P_{υ}					
	F-F		H-H		N-N	
	HO	AHO	HO	AHO	HO	AHO
0	9.88E-01	9.86E-01	1.0	1.0	9.99E-01	9.99E-01
1	1.17E-02	1.31E-02	5.63E-10	1.86E-09	1.11E-05	1.28E-05
2	1.39E-04	1.93E-04	3.17E-19	1.15E-17	1.23E-10	1.87E-10
3	1.66E-06	3.18E-06	1.78E-28	2.36E-25	1.37E-15	3.15E-15
4	1.97E-08	5.84E-08	1.00E-37	1.6E-32	1.52E-20	6.09E-20
5	2.35E-10	1.19E-09	5.64E-47	3.6E-39	1.69E-25	1.35E-24
6	2.79E-12	2.73E-11	3.18E-56	2.68E-45	1.88E-30	3.45E-29
N_{Tot}	1.0	1.0	1.0	1.0	1.0	1.0
$\boldsymbol{\upsilon}$	P_{υ}					
	H-F		N-O		C-O	
	HO	AHO	HO	AO	HO	AO
0	1.0	1.0	0.9999	0.999885	0.999972	0.999969
1	2.03E-09	4.84E-09	0.0001	0.000115	2.77E-05	3.15E-05
2	4.12E-18	5.59E-17	1.00E-08	1.51E-08	7.67E-10	1.13E-09
3	8.36E-27	1.54E-24	1.00E-12	2.27E-12	2.12E-14	4.59E-14
4	1.7E-35	1.01E-31	1.00E-16	3.91E-16	5.88E-19	2.13E-18
5	3.44E-44	1.59E-38	1.00E-20	7.73E-20	1.63E-23	1.12E-22
6	6.99E-53	5.94E-45	1.00E-24	1.75E-23	4.51E-28	6.7E-27
N_{Tot}	1.0	1.0	1.0	1.0	1.0	1.0

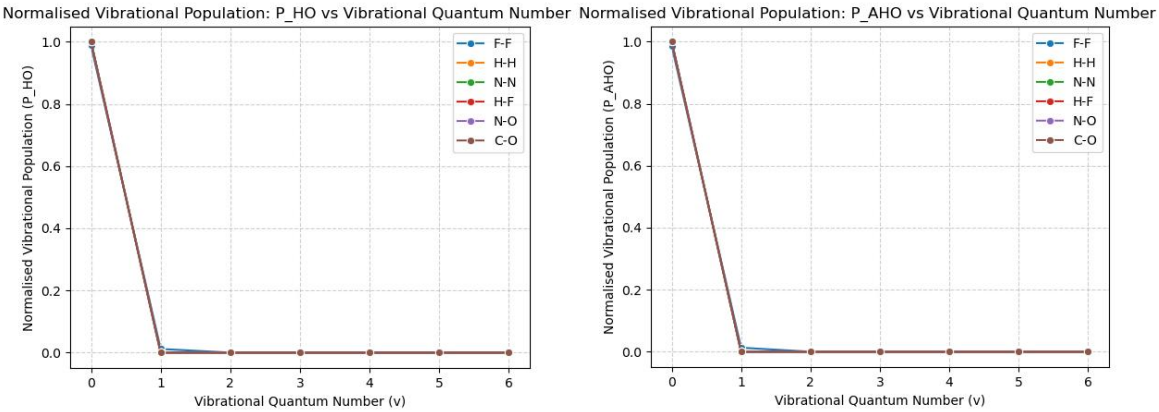

Fig.-2: Normalized Population Distribution of Different Molecules Against Vibrational Quantum Number ($\boldsymbol{\upsilon}$) for both HO and AHO Approximation

Population Distribution of Molecules among Various Rotational Levels in $\boldsymbol{\upsilon}$=0

The result mentioned in Table-6, as corroborated by Fig.-2, shows that the maximum number of molecules is present in the lowest vibrational level (υ = 0) for all the molecules at room temperature (298 K). Its value is almost 1. There are many rotational levels in each vibrational level. The rotational energy is given by eqn.-13.

$$E_{rot} = \widetilde{B}_{\upsilon} J\left(J+1\right) \qquad cm^{-1} \qquad (13)$$

The rotational constant $\breve{B}_v$ depends on v. $\breve{B}_0$ is determined from equation-14 and used to find J_{max} (equation-15).

$$\breve{B}_v = \breve{B}_e - \breve{\alpha}_e (v + 0.5) \quad cm^{-1} \qquad (14)$$

$$J_{max} = \sqrt{\frac{kT}{2hc\breve{B}_0}} - \frac{1}{2} \qquad (15)$$

Where $\breve{B}_e$ is a spectroscopic constant and $\breve{\alpha}_e$ is a rotational spectroscopic parameter (Table-7). $\breve{B}_0$ and J_{max} for diatomic molecules are computed using Python code (SI-Programme 5) and are given in Table-7.

Table-7: Rotational Constant $(\breve{B}_0)$ and J_{max} of Molecules at the Vibrational Level (v= 0)

Molecule	$\breve{B}_e/cm^{-1}$[2]	$\breve{\alpha}_e/cm^{-1}$ [2]	$\breve{B}_0/cm^{-1}$	J_{max}
$F^{19}-F^{19}$	0.8902	0.1385	0.820956.	10.721 ~ 11.0
$H^{1}-H^{1}$	60.8530	3.0622	59.3219	0.820 ~ 1.0
$N^{14}-N^{14}$	1.9982	0.0173	1.98955	6.708 ~ 7.0
$H^{1}-F^{19}$	20.9557	0.798	20.5567	1.742 ~ 2.0
$N^{14}-O^{16}$	1.6719	0.0171	1.66335	07.383 ~ 7.0
$C^{12}-O^{16}$	1.9313	0.0175	1.92255	6.832 ~ 7.0

The normalized (P_2) (equation-18) and unnormalized (P_1) (equation-19) rotational population is estimated using Python code (SI-Programme 6a-b) to observe the distribution of molecules among the rotational levels of the v =0 state only. The estimated values are plotted against rotational quantum number (J). The total number of rotational levels (equation-17) is chosen such a way that the sum of the normalized population of all the rotational levels becomes the same as that of v = 0 state.

$$N_{Tot}^{Rot} = \sum_{J=0}^{J_{final}} (2J+1) \exp\left(-\frac{hcJ(J+1)\breve{B}_0}{kT}\right) \qquad (17)$$

$$P\_2 = \frac{(2J+1)\exp\left(-\frac{hcJ(J+1)\breve{B}_0}{kT}\right)}{N_{Tot}^{Rot}} \qquad (18)$$

$$P\_1 \propto (2J+1)\exp\left(-\frac{hcJ(J+1)\breve{B}_0}{kT}\right) \qquad (19)$$

Normalized and unnormalized rotation populations are computed using Python code (SI-Programme 6a-d) and plotted against rotational quantum number, J, in Fig.-3a and Fig.-3b, respectively.

Table-8: Computed Values of Normalized and Unnormalized Rotational Population

Molecules									
	F-F			H-H			N-N		
Ground state(v=0)	J	P_1	P_2	J	P_1	P_2	J	P_1	P_2
Rotational Level	0	1	4.19E-3	0	1	2.60E-1	0	1	9.60E-3
J_{max} -1	10	13.568	5.69E-2	0	1	2.60E-1	6	8.678	8.33E-2
J_{max}	11	13.617	5.71E-2	1	1.690	4.40E-1	7	8.751	8.40E-2
J_{max} +1	12	13.456	5.64E-2	2	0.894	2.33E-1	8	8.502	8.16E-2
J_{final}	26	3.264	1.37E-2	6	7.59E-5	1.98E-5	26	6.17E-2	5.93E-4

N_{Tot}^{Rot}	1.0			1.0			1.0		
Molecules									
	H-F			N-O			C-O		
Ground state	J	P_1	P_2	J	P_1	P_2	J	P_1	P_2
Rotational Level	0	1	9.68E-2	0	1	8.04E-3	0	1	9.28E-3
J_{max} -1	1	2.459	2.38E-1	6	9.272	7.46E-2	6	8.796	8.16E-2
J_{max}	2	2.753	2.66E-1	7	9.559	7.69E-2	7	8.911	8.27E-2
J_{max} +1	3	2.122	2.05E-1	8	9.525	7.66E-2	8	8.703	8.07E-2
J_{final}	6	1.997E-1	1.93E-2	26	1.868E-1	1.50E-3	26	7.75E-2	7.19E-4
N_{Tot}^{Rot}	1.0			1.0			1.0		

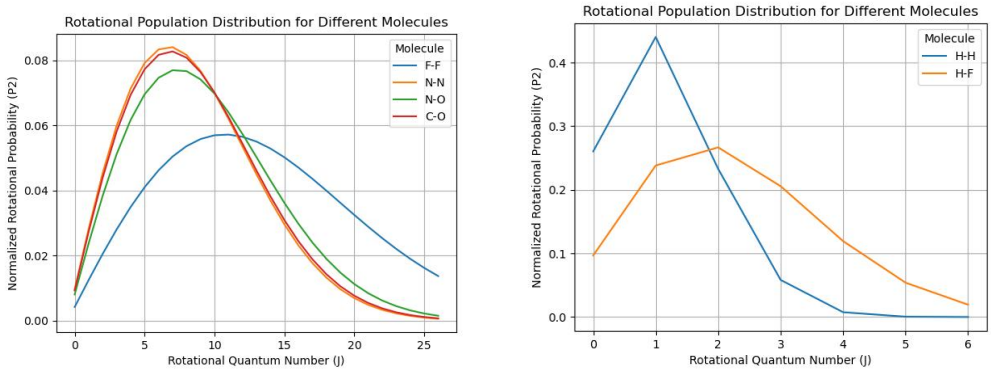

(a)

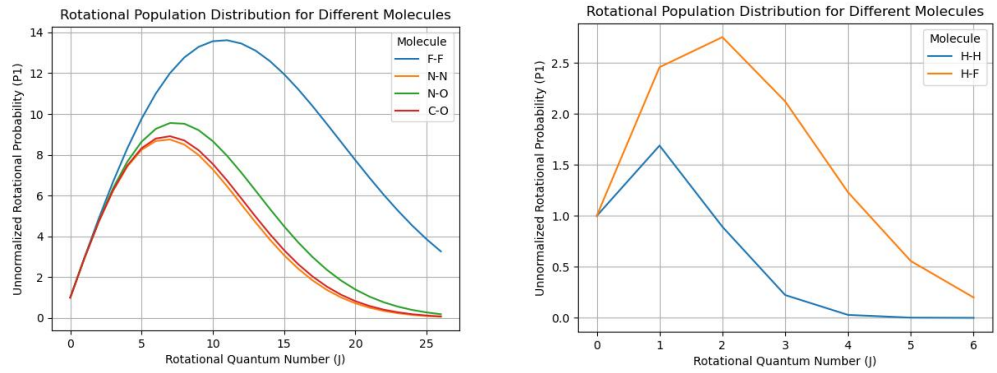

(b)

Fig.-3: Plot of (a) Normalized and (b) Unnormalized Rotational Population Density against Rotational Quantum Number, J, at $\boldsymbol{\nu} = 0$

Visualization of Wave Function and Probability Densities

The wave-function (equation-19) of the Harmonic oscillator is given as:

$$\psi_{\nu} = N_{\nu}\, H_{\nu}\left(\alpha^{0.5} x\right)\; e^{-\frac{\alpha x^2}{2}} \qquad (19)$$

Where N_{ν} is a normalisation constant (equation-20) and $H_{\nu}\left(\sqrt{\alpha}\, x\right)$ is the Hermite polynomials. The normalization constant is given by

$$N_{\nu} = \frac{1}{(2^{\nu}\nu!)^{\frac{1}{2}}} \left(\frac{\alpha}{\pi}\right)^{\frac{1}{4}} \qquad (20)$$

Where, $\alpha = (\frac{k\mu}{\hbar^2})^{\frac{1}{2}}$, k = force constant, μ = reduced mass of the molecule. The wave functions for a few vibrational levels are listed in Table-9.

Table-9: Harmonic-Oscillator wavefunctions.

ν	Ψ_ν
0	$(\frac{\alpha}{\pi})^{\frac{1}{4}} \quad e^{\frac{-\alpha x^2}{2}}$
1	$(\frac{4\alpha^3}{\pi})^{\frac{1}{4}} \quad x\ e^{\frac{-\alpha x^2}{2}}$
2	$(\frac{\alpha}{4\pi})^{\frac{1}{4}} \quad (2\alpha x^2 - 1) \quad e^{\frac{-\alpha x^2}{2}}$
3	$(\frac{\alpha^3}{9\pi})^{\frac{1}{4}} \quad (2\alpha x^3 - 3x)\ e^{\frac{-\alpha x^2}{2}}$
4	$(\frac{\alpha}{36\pi})^{\frac{1}{4}} (4\alpha^2 x^4 - 12\alpha x^2 + 3) \quad e^{\frac{-\alpha x^2}{2}}$
5	$(\frac{1}{60})^{\frac{1}{2}} (\frac{\alpha^3}{\pi})^{\frac{1}{4}} (4\alpha^2 x^5 - 20\alpha x^3 + 15x)\ e^{\frac{-\alpha x^2}{2}}$
6	$\frac{1}{12} (\frac{\alpha}{25\pi})^{\frac{1}{4}} (8\alpha^3 x^6 - 60\alpha^2 x^4 + 90\alpha x^2 - 15) e^{\frac{-\alpha x^2}{2}}$

The computed energy, wave function, and probability densities of the molecules are tabulated in Table-8. As can be seen from the data, these three parameters vary extensively in both magnitude and units. The energy and probability density are positive quantities, whereas the amplitude of the wave function oscillates between positive and negative, except for ν=0 state. Hence, it becomes difficult to plot the wave function and probability density together at their corresponding energy levels without using different scales. To address this challenge, a computational normalization procedure was implemented. The wave functions and probability densities were appropriately scaled and aligned with their corresponding vibrational energy levels. This approach enables simultaneous visualization of these quantities without requiring multiple axes. The resulting plots clearly demonstrate how the wave function changes with increasing vibrational quantum number. As the value of v increases, the number of nodes in the wave function increases accordingly. The probability density distribution also becomes broader, indicating a larger spatial spread of the vibrational motion. Special effort has been made during renormalization of the wave function to ensure that the mean of oscillation coincides with the corresponding energy level, while maintaining a probabilistic character.

Table-10: Wave Function (Ψ) and Probability Density (Ψ^2) of the F-F Molecule at ν=1

F-F (E_1 = 1374 cm^{-1})						
l/pm	Ψ	$\Psi_{modified}$	$E_1 + \Psi_{modified}$	Ψ^2	$\Psi_{modified}^2$	$E_1 + \Psi_{modified}^2$
101.19	-4E-09	-4E-06	1374	1.64E-17	2.46E-13	1374
135.19	-0.25671	-256.71	1117.289	0.065901	988.5088	2362.509
140.19	-0.06673	-66.7325	1307.268	0.004453	66.79836	1440.798
141.19	-1.5E-13	-1.5E-10	1374	2.36E-26	3.54E-22	1374
142.19	0.066732	66.732	1440.732	0.004453	66.79836	1440.798
147.19	0.256711	256.711	1630.711	0.065901	988.5088	2362.509
181.19	4.05E-09	4.05E-06	1374	1.64E-17	2.46E-13	1374

The Python code for the four molecules F-F, N-N, C-O, and H-F is given in SI-Programmes 6a, 6b, 6c, and 6d, respectively. To have a better understanding of the same, data computed using SI-Programme 6a for F-F is tabulated in Tables-10 and 11 and is used for plotting Fig.-4, keeping $\boldsymbol{\nu}$ =1 and 6. The

corresponding data for other molecules are given in Table-SI-1-6, and corresponding plots for wave function and probability density are given in Figs.-5 to 7.

Table-11: Wave Function (Ψ) and Probability Density (Ψ^2) of the F-F Molecule at υ=6

F-F (E_6 = 5954 cm^{-1})						
l/pm	Ψ	$\Psi_{modified}$	$E_6 + \Psi_{modified}$	Ψ^2	$\Psi_{modified}^2$	$E_6 + \Psi_{modified}^2$
101.19	7.38E-06	7.38E-03	5954.007	5.45E-11	8.18E-07	5954
121.19	0.215202	215.2016	6169.202	0.046312	694.6757	6648.676
126.19	0.021139	21.13895	5975.139	0.000447	6.702829	5960.703
127.19	-0.06205	-62.0497	5891.95	0.00385	57.75241	6011.752
130.19	-0.17522	-175.217	5778.783	0.0300701	460.5162	6414.516
132.19	-0.05648	-56.4771	5897.523	0.00319	47.84495	6001.845
133.19	0.035276	35.27559	5989.276	0.001244	18.66551	5972.666
135.19	0.164445	164.4451	6118.445	0.027042	405.6331	6359.633
138.19	0.02526	25.26022	5979.26	0.000638	9.571183	5963.571
139.19	-0.06869	-68.6899	5885.31	0.004718	70.77456	6024.775
141.19	-0.16763	-167.628	5786.372	0.028099	421.486	6375.486
143.19	-0.06869	-68.6899	5885.31	0.004718	70.77456	6024.775
144.19	0.02526	25.26022	5979.26	0.000638	9.571183	5963.571
149.19	0.035276	35.27559	5989.276	0.001244	18.66551	5972.666
150.19	-0.05648	-56.4771	5897.523	0.00319	47.84495	6001.845
152.19	-0.17522	-175.217	5778.783	0.030701	460.5162	6414.516
155.19	-0.06205	-62.0497	5891.95	0.00385	57.75241	6011.752
156.19	0.0211139	21.13895	5975.139	0.000447	6.702829	5960.703
160.19	0.220498	220.4978	6174.498	0.048619	729.2894	6683.289
181.19	7.38E-06	0.007385	5954.007	5.45E-11	8.18E-07	5954

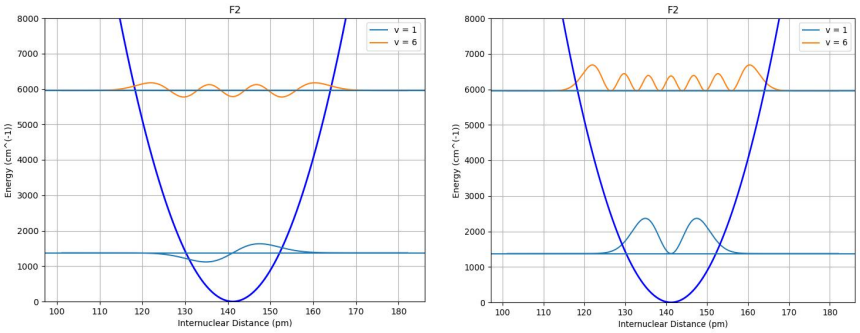

Fig.-4: Wave Functions (Ψ) and Probability Densities (Ψ^2) of the F-F Molecule at υ=1 and 6 Plotted against Internuclear Distance l/(pm).

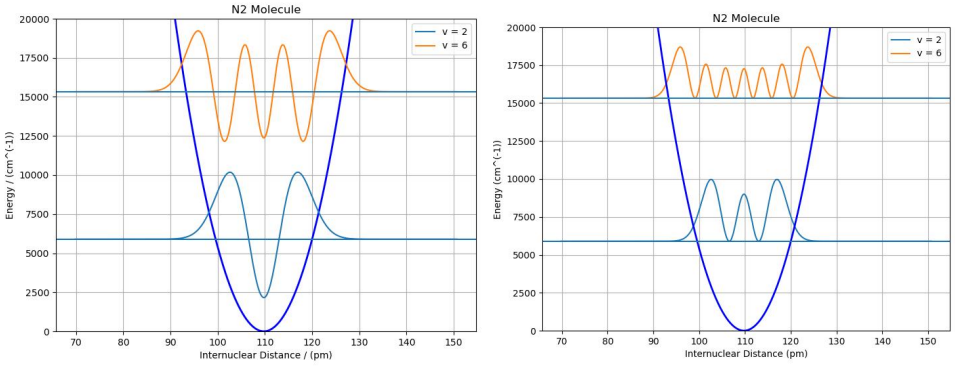

Fig.-5: Wave Functions (Ψ) and Probability Densities (Ψ^2) of the N-N Molecule at υ=2 and 6 Plotted against Internuclear Distance l/(pm)

The vibrational quantum numbers are varied for each diatomic molecule to understand their effects on the wavefunction and probability density. This integrated visualization technique provides a clearer physical interpretation of the quantum mechanical behaviour of vibrating molecules. By simultaneously displaying energy levels, wave functions, and probability densities, the graphical representation enhances conceptual understanding of vibrational dynamics in diatomic molecules.

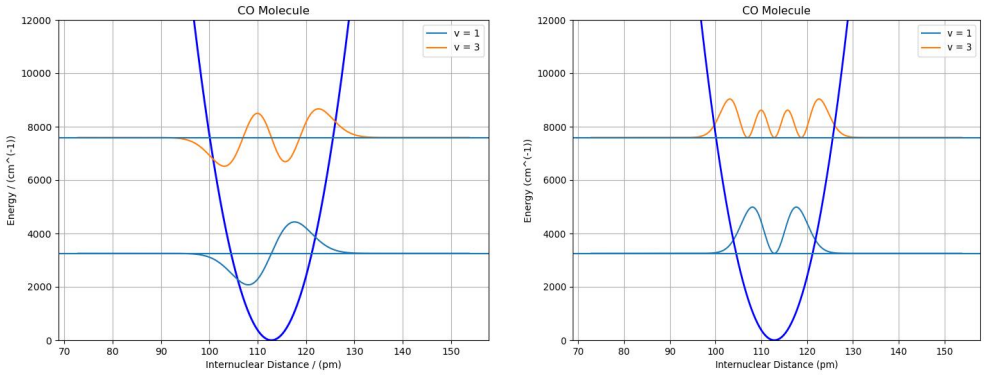

Fig.-6: Wave Functions (Ψ) and Probability Densities (Ψ^2) of the C-O Molecule at υ=1 and 3 Plotted Against Internuclear Distance l/(pm).

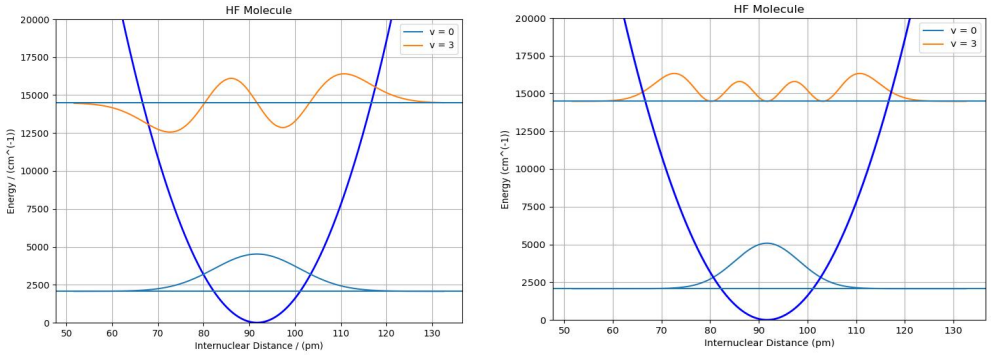

Fig.-7: Wave Functions (Ψ) and Probability Densities (Ψ^2) of the H-F Molecule at υ=0 and 3 Plotted against Internuclear Distance l/(pm).

CONCLUSION

The present study demonstrates the effective use of Python-based computational methods to analyze vibrational and rotational characteristics of selected diatomic molecules, including F–F, H–H, N–N, H–F, N–O, and C–O. Using molecular constants obtained from spectroscopic data, vibrational energy levels for both harmonic and anharmonic oscillators were calculated, along with maximum vibrational quantum numbers and Boltzmann population distributions. The results highlight the limitations of the harmonic oscillator model and emphasize the importance of anharmonic corrections for accurately describing molecular vibrations. In addition, the rotational population distributions in the ground vibrational state were evaluated, providing further insight into molecular energy distributions. A key outcome of this work is the development of a graphical approach that simultaneously represents vibrational energy levels, wave functions, and probability densities on a common scale despite their different physical units. This visualization enhances the interpretation of quantum mechanical concepts that are often difficult to understand through equations alone. Furthermore, the integration of computational tools such as Python in quantum chemistry education supports Sustainable Development Goal 4 (Quality Education) by promoting digital learning, computational literacy, and improved conceptual understanding in modern chemical education. The approach presented here not only provides insight into the vibrational and rotational characteristics of diatomic molecules but also serves as a useful pedagogical tool for improving conceptual understanding of quantum mechanics in chemical education.

ACKNOWLEDGMENTS

We would like to thank Prof Baljeet Kaur, Department of Computer Science, for her insightful and valuable suggestions that enhanced the manuscript.

CONFLICT OF INTERESTS

The authors declare that there is no conflict of interest.

AUTHOR CONTRIBUTIONS

The present work is related to *SDG-4: Quality Education*. All the authors contributed significantly to this manuscript, participated in reviewing/editing and approved the final draft for publication. The research profile of the authors can be verified from their ORCID ids, given below:

Jyoti Singh https://orcid.org/0000-0003-4108-3861
Vansh Wadhwa https://orcid.org/0009-0008-6989-0394
Shampa Bhattacharyya https://orcid.org/0000-0001-6712-5375

Cite this article as: J. Singh *et al.*, *Rasayan J. Chem.*, 19(2), 1017-1028(2026), https://doi.org/10.31788/RJC.2026.1929626.

REFERENCES

1. D. J. Griffiths, Introduction to Quantum Mechanics *(*2nd ed.), *Pearson Prentice Hall*, (2005), https://doi.org/10.1017/9781316995433
2. D. A. McQuarrie, Quantum Chemistry, *University Science Books*, (2008). https://search-library.ucsd.edu/permalink/01UCS_SDI/1iecivl/alma9910027453797065 35
3. R. Shankar, Principles of Quantum Mechanics (2nd ed.), *Springer*, (1994), https://doi.org/10.1007/978-1-4757-0576-8
4. M. V. Staveren, *Journal of Chemical Education*, **99**, 2604(2022), https://doi.org/10.1021/acs.jchemed.2c00193
5. A.R. McDonald and J.A. Nash, Teaching Programming across the Chemistry Curriculum, In *ACS Symposium Series*, (2021), https://doi.org/10.1021/bk-2021-1387
6. A.R. Leach, Molecular Modelling: Principles and Applications (2nd ed.), *Pearson Education: Harlow*, 2001, https://www.worldcat.org/isbn/9780582382107
7. W.B. Jensen, Introduction to Computational Chemistry (3rd ed), *Wiley: Chichester,* (2017), https://www.wiley.com/en-in/Introduction+to+Computational+Chemistry%2C+3rd+Edition-p-9781118825952
8. P.Virtanen, R. Gommers, T.E. Oliphant, M. Haberland, T. Reddy, D. Cournapeau, E. Burovski, P. Peterson, W. Weckesser, J. Bright, S.J. Van Der Walt, M. Brett, J.Wilson, K.J. Millman, N. Mayorov, A.R.J. Nelson, E. Jones, R. Kern, E. Larson, C.J. Carey, I. Polat, Y. Feng, E.W. Moore, J. VanderPlas, D. Laxalde, J. Perktold, R. Cimrman, I. Henriksen, E.A. Qintero, C.R. Harris, A.M. Archbald, A.H. Ribeiro, F. Pedregosa, P. van Mulbregt and T. Pudlik, *Nature Methods,* **17(3)**, 261(2020), https://doi.org/10.1038/s41592-019-0686-2
9. J. D. Hunter, *Computing in Science & Engineering*, **9(3)**, 90(2007), https://doi.org/10.1109/MCSE.2007.55
10. C. N. Banwell and E.M. McCash, Fundamentals of molecular spectroscopy (4th ed.), McGraw-Hill, (1994), https://search.worldcat.org/title/29753560

[RJC-9626/2026]